

# Theoretical analysis and experimental verification of a cost-effective chromatic dispersion monitoring method in a 40-Gb/s optical fiber communication system

Yan Li (李岩), Jin Zhang (章锦), Jinlong Yu (于晋龙),  
Wencai Jing (井文才), Yimo Zhang (张以谟), and Ge Zhou (周革)

*College of Precision Instrument & Opto-Electronics Engineering;*

*Key Laboratory of Opto-Electronics Information and Technical Science, Ministry of Education;*

*Laboratory of Optical Fiber Communication, Tianjin University, Tianjin 300072*

Received June 7, 2005

A cost-effective technique for in-service chromatic dispersion monitoring in a 40-Gb/s optical communication system is proposed. Microwave devices are adopted to detect the electrical power of a specific frequency band. A simplified theoretical model is proposed and discussed focusing on the relationship between electrical power and chromatic dispersion at different frequency bands. The dynamic monitoring of chromatic dispersion is achieved using devices such as PIN detector, microwave amplifier, narrow-band microwave filter, and electrical power detector. The maximum detectable chromatic dispersion is 130 ps/nm and a resolution of 5.2 ps/nm/dB has been achieved in the frequency band centered at 12 GHz.

OCIS codes: 060.2330, 260.2030, 350.4010.

Dynamic and tunable chromatic dispersion compensation technique is one of the essential features of 40-Gb/s optical fiber transmission systems. The tolerable residual chromatic dispersion for 40-Gb/s transmission system is only 60 ps/nm or even less<sup>[1]</sup>. At the same time, chromatic dispersion varies due to network reconfigurations, temperature fluctuation, and laser's wavelength drift, etc.<sup>[2]</sup>. Therefore, it is necessary to apply a simple and effective method for monitoring the residual chromatic dispersion in transmission. Thus the tunable chromatic dispersion compensators in the systems could be tuned accordingly and operated dynamically.

Various chromatic dispersion monitoring techniques have been reported, including: 1) general performance monitoring using eye-opening diagram,  $Q$ -factor, on/off ratio, or bit-error rate (BER)<sup>[3,4]</sup>; 2) adding a subcarrier tone and detecting phase or power change<sup>[5-8]</sup>; 3) extracting clock component at the receiver and detecting the change of phase or RF power<sup>[9,10]</sup>; 4) measuring the phase delay of double sideband tone<sup>[1]</sup>; 5) inserting chromatic dispersion sensitive devices (nonlinear optical fiber, photon-counting Si avalanche diode (APD) or semiconductor optical amplifier (SOA))<sup>[11-13]</sup>. However, the second approach is not suitable for practical optical fiber transmission systems since it requires extraneous signals added to the base-band at transmitter. And other techniques mentioned above need to employ at least one of the expensive devices such as high-speed bit error rate tester (BERT), high-speed phase detector, high-speed clock recovery circuits, etc.. The costs of these components would increase sharply with the speed of the system beyond 10 Gb/s.

In this paper, a novel and cost-effective chromatic dispersion monitoring method for single-channeled fiber link is proposed. This method is simple to realize by detecting the electrical power of a specific frequency band of the transmitted signal output by the photo-detector and

it can realize online monitoring. A tuning range of 130 ps/nm and a solution of 5.2 ps/nm/dB are achieved in the experiments, which are subservient for chromatic dispersion compensation systems. The detecting circuits used in the experiment guarantee that the response speed of the feedback signal is quick enough for controlling tunable dispersion compensators (TDCs) in 40-Gb/s fiber systems. Therefore, the requirements of chromatic dispersion monitoring at 40 Gb/s are satisfied.

Chromatic dispersion changes the phase of each frequency component and broadens optical signal pulses in time domain, while not changing the optical power spectrum. The electrical power monitoring is to detect the electrical power of a specific frequency band of the electric signals put out by photo-detector. The photo-detector converts optical pulses into electrical pulses. The converted electrical signals only reflect the power of the optical pulses in time domain, while ignoring the phase changes. Therefore, as chromatic dispersion broadens the input optical pulses in time domain, the output electrical signal pulses also broaden in time domain accordingly, but narrow in frequency domain, then the electrical power of a given frequency band will change according to the online chromatic dispersion.

The electrical spectrum is also influenced by the loss and nonlinear effect in the optical fiber transmission systems. The loss can be compensated by erbium-doped fiber amplifiers (EDFAs). As the optical power in single channel 40-Gb/s transmission systems is on the order of micro watt magnitude, the influence of nonlinear effect can be ignored.

Take Gaussian pulses, which are widely transmitted in optical fiber communication systems, for example, the function of the original amplitude envelope is

$$A(0, T) = \exp\left(-\frac{T^2}{2T_0^2}\right). \quad (1)$$

When residual chromatic dispersion reaches  $d$  (ps/nm), the above function comes to be

$$A(d, T) = \left( \frac{T_0^2}{T_0^2 + j \frac{\lambda^2 d}{2\pi c}} \right)^{1/2} \exp \left[ -\frac{T^2}{2 (T_0^2 + j \frac{\lambda^2 d}{2\pi c})} \right]. \quad (2)$$

Taking out the phase component in Eq. (2), we get

$$I(d, t) = |A(d, T)| = \frac{T_0}{\sqrt[4]{T_0^4 + \frac{\lambda^4 d^2}{4\pi^2 c^2}}} \exp \left[ -\frac{T^2 T_0^2}{2 (T_0^4 + \frac{\lambda^4 d^2}{4\pi^2 c^2})} \right]. \quad (3)$$

In Eqs. (1)—(3),  $T$  is the time domain measurement of the reference system that moving with the pulses at the speed of group velocity;  $T_0$  is the initial pulse width of Gaussian pulse;  $\lambda$  is the center wavelength;  $d$  is the amount of chromatic dispersion, and  $c$  is the velocity of light in vacuum.

So, the spectrum of photo-detector output signal is

$$S(\omega) = |F[I(d, t)]|, \quad (4)$$

where arithmetic operator  $F[.]$  represents Fourier transformation.

The optical signals transmitted in fiber links are dualistic random code. Supposed the code element period is  $T_1$ , the power spectrum could be described using the following equation

$$P(\omega) = \frac{|S(\omega)|^2}{4T_1} \left[ 1 + \frac{2\pi}{T_1} \sum_{n=-\infty}^{\infty} \delta \left( \omega - \frac{2\pi n}{T_1} \right) \right]. \quad (5)$$

It is shown in Eq. (5) that the dualistic random code only influences the electrical power density at clock frequency components or multiple clock frequency components. Components at other frequency do not change. Therefore, any frequency band that does not include components at clock frequency and multiple clock frequency can be monitored as a feedback signal for chromatic dispersion monitoring.

Figure 1(a) describes the shape of Gaussian pulses in time domain, Fig. 1(b) shows the electrical spectra of Gaussian pulses. In Fig. 1, the solid line, dash-dot line, and the dotted line represent the pulses under the condition that the chromatic dispersion is 0, 68, and 136 ps/nm, respectively. The initial Gaussian pulse width (FWHM) is 15 ps in the figure. From Fig. 1, we can see that the chromatic dispersion results in both the narrowing of the electrical spectrum and the electrical power change of frequency components.

It is needed to choose the appropriate frequency band for chromatic dispersion monitoring, that is to choose the eligible center frequency and bandwidth. If the bandwidth is narrow enough, curves of normalized electrical power density via chromatic dispersion under the center frequency can be used to reflect the relationship between

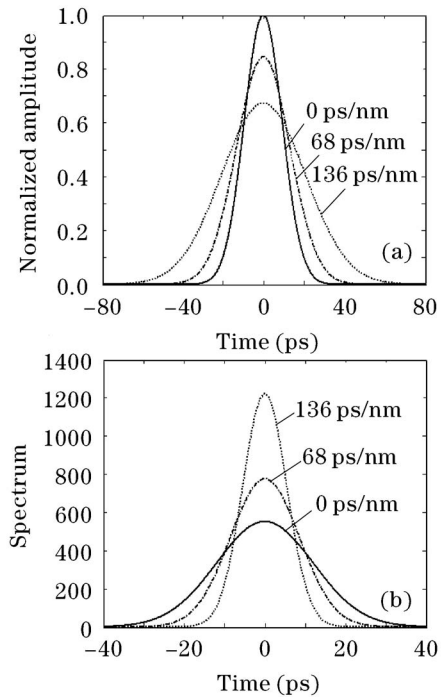


Fig. 1. Gaussian pulse shapes (a) and electrical spectra of the pulses (b) under chromatic dispersions of 0, 68, and 136 ps/nm.

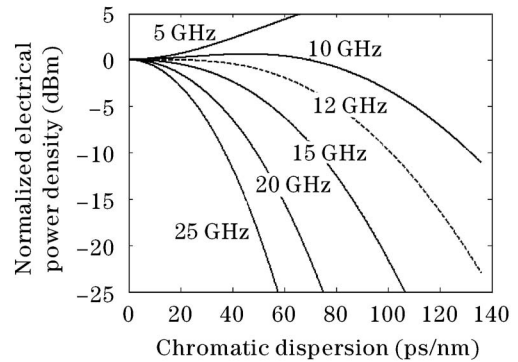


Fig. 2. Normalized electrical power via chromatic dispersion under frequency components of 5, 10, 12, 15, 20, and 25 GHz.

the electrical power of the frequency band and the chromatic dispersion to choose the center frequency, curves of normalized electrical power density via chromatic dispersion under frequency components of 5, 10, 12, 15, 20, and 25 GHz are calculated respectively (see Fig. 2). Consider the situation shown in Fig. 2, when the frequency of the component rises, the measuring range increases and the electrical power diminishes. The lessened electrical power is difficult to detect. We have to take a trade off between measuring accuracy and system cost. By calculation we get the monitoring range of 130 ps/nm and the average measuring resolution of 5.2 ps/nm/dB at 12-GHz frequency component. 5.2 ps/nm/dB means that a 5.2 ps/nm chromatic dispersion change will give raise to  $-1$ -dB electrical power change in the electrical monitor signal. The electrical power fades  $-20$  dB at the monitoring range of 130 ps/nm. Thus the frequency component at 12 GHz (avoiding clock frequency and multiple clock frequency

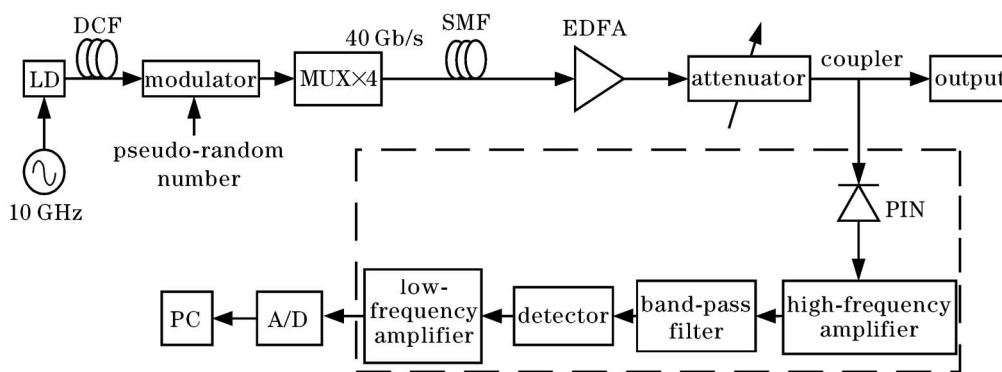


Fig. 3. Experimental setup of chromatic dispersion monitoring.

components) is considered to be appropriate for the chromatic dispersion detection in 40-Gb/s systems.

Apparently, the shape of curves in the above figure change with different pulse shapes. When the pulse shape is fixed, the curve shape keeps the original states. As a result, by choosing the appropriate frequency band, the method proposed in this paper can also be applied in other situations with transmission pulses of different shapes.

The experimental setup of chromatic dispersion monitoring is shown in Fig. 3. The devices in the dashed rectangular are the electrical power detecting circuits.

The optical source is amplitude modulated to generate 10-GHz optical pulses. The center wavelength of the laser is 1550 nm with line width of 0.4 nm. Then the pulse width (FWHM) is compressed to 15 ps using dispersion compensation fiber (DCF) connected to the laser. And the compressed optical pulses are modulated to generate 10-Gb/s return-to-zero (RZ) pseudo-random codes. Before launching into the fiber link, 40-Gb/s RZ pseudo-random data stream is generated by time domain multiplexing  $4 \times 10$ -Gb/s signals using a time-division multiplexer.

Coils of single mode fiber (SMF) are employed to simulate chromatic dispersion in practical link, and the dispersion varies with the length of SMF connected. The SMF used in this experiment has a dispersion coefficient of 17 ps/nm/km, a loss coefficient of 0.3 dB/km, and a nonlinear coefficient of  $1.5 \text{ (W/km)}^{-1}$ . The nonlinear effect induces a negligible penalty to experimental results. However the loss of the optical signals changes with the fiber length and causes the detected electrical power to fade accordingly. To compensate the loss resulting from SMF, the EDFA is employed. To make the average optical power received by photo-detector be the same when the SMF length varies, a tunable attenuator is launched ahead of the detector. By use of the EDFA and the tunable attenuator, the monitoring system is independent of the power of optical signals.

The electrical power detecting circuits are realized by the PIN photodiode, the microwave power amplifier, the microwave filter, and the power detector connected in series. The PIN photodiode employed has the bandwidth of 35 GHz with 0.7-A/W optical responsibility. The parameters of the microwave power amplifier are given as

following. The center frequency is at 12 GHz, the bandwidth is 200 MHz, the gain is 30 dB, and the noise is less than 1.5 dB. The microwave band-pass cavity filter has center frequency of 12 GHz, bandwidth of 100 MHz and insertion loss of  $< 2$  dB. Actually, the bandwidth (0.1 GHz) of the cavity filter is just as small as 0.8% of the center frequency (12 GHz), so the influence of the filter bandwidth on the relationship between the electrical power and chromatic dispersion can be left out of account. The microwave power detector with voltage sensitivity of  $0.8 \text{ mV}/\mu\text{W}$  is used to convert input power into voltage signal. The output low frequency voltage signal is firstly amplified by a low frequency amplifier, then sampled by an A/D converter and finally sent to the computer to get the chromatic dispersion in the link.

The response time of the whole system is mainly dependent on the A/D converter. The sampling rate of the A/D converter used in the experiment is 4.5 k/s. So the response time is  $222 \mu\text{s}$ , which is quick enough for controlling TDCs in 40-Gb/s fiber systems.

Electrical power and eye diagram are measured under different chromatic dispersions. Figure 4 illustrates the normalized electrical power of the frequency band centered at 12 GHz as a function of the chromatic dispersion. The dots in figure stand for experimental results, and the solid line is theoretically simulated curve calculated by Eq. (4). It can be seen in Fig. 4 that the experiment results agree well with the theoretical analysis. Figure 5 displays the eye diagrams of 40-Gb/s RZ signal

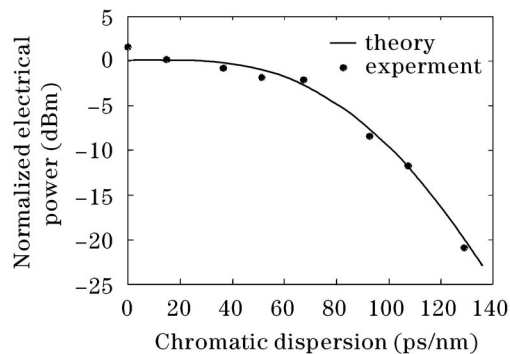


Fig. 4. The normalized electrical power of the frequency band centered at 12 GHz as a function of chromatic dispersion.

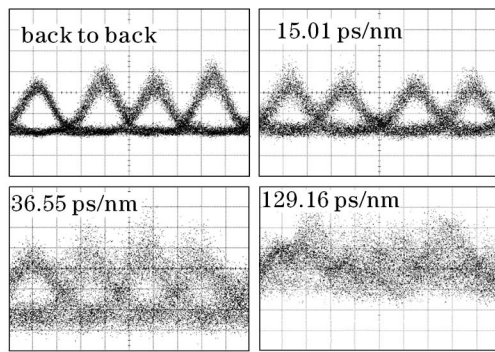


Fig. 5. Eye-diagram of 40-Gb/s RZ signal with different residual chromatic dispersions.

when chromatic dispersion is 0, 15.01, 36.55, and 129.16 ps/nm. The pulse signals distort seriously when residual chromatic dispersion reaches 129.16 ps/nm.

In conclusion, an online chromatic dispersion monitoring method for single-channelled 40-Gb/s optical fiber transmission system is proposed in this paper. Under the condition of Gaussian pulses, theoretical analysis is given to demonstrate the relationship between electrical power of different frequency components and chromatic dispersion. In the experiment, we adopted tools like PIN detector, microwave amplifier, narrow-band microwave filter, and power detector to monitor the electrical power under frequency band centered at 12 GHz that we choose as the appropriate frequency band. The electrical power with chromatic dispersion ranging from 0 to 129.16 ps/nm is recorded and experimental results agree with the theoretical analytical results.

This work was supported by the National Natural Science Fund of China (No. 60377031), and the National Basic Research Program of China (No. 2003CB314907).

Y. Li's e-mail address is thisliyan@hotmail.com.

## References

1. Q. Yu, Z. Pan, L.-S. Yan, and A. E. Willner, *J. Lightwave Technol.* **20**, 2267 (2002).
2. A. E. Willner, in *Proceedings of LEOS'2002* Tu11, 201 (2002).
3. T. Sugihara, K. Shimomura, K. Shimizu, Y. Kobayashi, K. Matsuoka, M. Hashimoto, T. Hashimoto, T. Hirai, S. Matsumoto, T. Ohira, M. Takabayashi, K. Yoshiara, and T. Mizuochi, in *Proceedings of OFC'2002* ThAA2, 577 (2002).
4. Y. Yokoyama, T. Ito, and K. Fukuchi, in *Proceedings of ECOC'2003* Tu 4.2.1 (2003).
5. T. E. Dimmick, G. Rossi, and D. J. Blumenthal, *IEEE Photon. Technol. Lett.* **12**, 900 (2000).
6. K. J. Park, C. J. Youn, J. H. Lee, and Y. C. Chung, in *Proceedings of OFC'2002* ThGG88, 735 (2002).
7. M. N. Petersen, Z. Pan, S. Lee, S. A. Havstad, and A. E. Willner, *IEEE Photon. Technol. Lett.* **14**, 570 (2002).
8. Y. Takushima and K. Kikuchi, *Electron. Lett.* **37**, 743 (2001).
9. Z. Pan, Y. Xie, S. A. Havstad, Q. Yu, A. E. Willner, V. Grubsky, D. S. Starodubov, and J. Feinberg, *Opt. Commun.* **230**, 145 (2004).
10. T. Inui, T. Komukai, M. Nakazawa, K. Suzuki, K. R. Tamura, K. Uchiyama, and T. Morioka, *IEEE Photon. Technol. Lett.* **14**, 549 (2002).
11. S. Wielandy, M. Fishteyn, T. Her, D. Kudelko, and C. Zhang, in *Proceedings of OFC'2003* TuD5, 166 (2003).
12. P. S. Westbrook, B. J. Eggleton, T. Her, G. Raybon, and S. Hunsche, in *Proceedings of OFC'2002* WU6, 335 (2002).
13. P. S. Westbrook, B. J. Eggleton, G. Raybon, S. Hunsche, and T. Her, *IEEE Photon. Technol. Lett.* **14**, 346 (2002).